Kondo Sidebands in CeAl$_3$ and Related Pseudobinary Compounds

K. H. J. Buschow, H. J. van Daal, F. E. Maranzana, and P. B. van Aken

Philips Research Laboratories, N. V. Philips' Gloeilampenfabrieken,

Eindhoven, Netherlands

The temperature dependence of the electrical resistivity (1.3–300 °K) has been studied for the isomorphous compounds Ce$_{1-x}$La$_x$Al$_3$, Ce$_{1-x}$Y$_x$Al$_3$, and Ce$_{1-x}$Th$_x$Al$_3$. In these compounds, one or two maxima have been observed in the ρ-vs-T curve. An analysis of the experimental results is presented in terms of the Kondo sideband theory, which describes Kondo exchange scattering of the conduction electrons in the presence of localized moments whose ground-state manifold is split owing to the presence of crystalline fields. It is shown that the changes observed in ρ behavior for CeAl$_3$ upon replacement of Ce by La, Y, or Th can be correlated with changes in the crystal field parameters, and in the case of Th also with changes in the density of states of the conduction electrons.

I. INTRODUCTION

Anomalous behavior of the temperature dependence of the electrical resistivity ρ has been observed recently in some cerium-aluminium compounds, viz., CeAl$_2$ [1] and Ce$_3$Al$_{11}$.[2] In these compounds, ρ shows a gradual rise with decreasing temperature below about 15 and 20 °K, a sharp maximum at 4.5 and 6 °K, followed by a marked fall. The gradual rise of ρ was interpreted as being due to Kondo exchange scattering. The maximum was attributed to the onset of magnetic-ordering effects, quenching the Kondo exchange-scattering mechanism. The sharp fall of ρ was thought to be due to the disappearance of the Kondo effect and to the decrease of normal spin-disorder scattering.

In the compound CeAl$_3$, a marked rise of ρ was found with decreasing temperature, starting not far below room temperature.[3] At about 35 °K, the ρ-T curve reaches a maximum and then, below this temperature, falls rapidly. This latter behavior cannot be ascribed to magnetic-ordering effects. Magnetic measurements have shown that these effects are absent in the relevant temperature region. It has already been suggested[3] that in CeAl$_3$, just as in CeAl$_2$ and Ce$_3$Al$_{11}$, the Kondo effect is active, and assumes giant proportions in this compound. The conditions in CeAl$_3$ are indeed favorable for the occurrence of such an effect. It has been found from magnetic measurements and from data for the lattice constants that the Ce ions are in the trivalent state and thus carry a localized moment. Furthermore, it follows from Knight-shift data for the NMR of Al^{27} [4,5] that the effective s-f exchange integral has a high negative value. However, attempts to explain the observed ρ behavior in CeAl$_3$ by means of traditional second-order perturbational Kondo theory failed. It is suggested in the present paper that the reason for the failure is connected with the fact that in Kondo's theory the localized

spin moment is considered to remain unchanged with temperature (apart from a repopulation of the Zeeman levels due to the possible presence of a weak internal field). In compounds such as CeAl$_3$, crystalline electric fields are operative which bring about a variation of the localized Ce^{3+} moment with temperature. The Kondo sideband model recently proposed by Maranzana[6] for the resonance scattering of conduction electrons takes account of the presence of crystalline electric fields.

It is the purpose of the present paper to show that the experimental ρ-vs-T curves given for CeAl$_3$ and the related pseudobinary compounds in Sec. II strongly support the validity of the Kondo sideband model. First, in Sec. III, an outline is given of the nature of the crystal field splitting in CeAl$_3$ and the changes introduced in the latter upon partial replacement of Ce by La, Y, or Th. Moreover, the substitution of Th for Ce affects the electronic density of states at the Fermi level. The main features of the Kondo sideband model are outlined in Sec. IV. In Sec. V, an interpretation of ρ data is presented on the basis of the Kondo sideband model, taking into account variations of the crystal field parameters and of the electronic density of states. A discussion of this interpretation can be found in Sec. VI.

II. EXPERIMENTAL

The samples have been prepared by arc melting followed by vacuum annealing (3 weeks at 900 °C); the purity of the rare-earth metals was 99.9%, that of aluminium 99.99%. The compounds CeAl$_3$, LaAl$_3$, α-YAl$_3$, and ThAl$_3$ are isostructural and have the hexagonal Ni$_3$Sn structure.[7] X-ray diffraction showed that a continuous region of solid solution exists between any two of these compounds, that is to say, the sets of pseudobinary compounds Ce$_{1-x}$, Th$_x$Al$_3$, Ce$_{1-x}$La$_x$Al$_3$, and Ce$_{1-x}$Y$_x$Al$_3$ studied in this

investigation were found to be isostructural. The binary compound YAl_3 when not alloyed with $CeAl_3$, $LaAl_3$, or $ThAl_3$ could be obtained by us as a single-phase compound only in its rhombohedral β modification, which is a stacking variant of the α form. The lattice constants of the binary compounds are given in Table I. The lattice constants of the pseudobinary compounds can be obtained from a linear interpolation between the data of the relevant binary compounds (Vegard's law).

The resistivity data have been obtained in the temperature range 1.3–300 °K by the same method as described before.[8] The results for the three sets of compounds are shown in Figs. 1–3. It is seen that in nearly all cases the resistivity still decreases markedly in the vicinity of the lowest measuring temperature, making an estimate of its residual part impossible. As we are especially interested in the variation of ρ with temperature, we have subtracted a constant value from each curve such that the ρ-T curves of compounds belonging to the same set match at 300 °K. It is seen from the figures that partial replacement of Ce by the nonmagnetic elements La, Y, or Th leads to significant changes in the temperature dependence of ρ. The salient feature of the experimental resistivity curves is the presence of one or two peaks. The position of these peaks on the temperature scale depends on the nature and on the molar fraction of the substituent. The constituent elements of the compounds under consideration are trivalent with the exception of Th which is tetravalent. Therefore, substitution of Th for Ce might lead to appreciable changes in the density of states of the conduction electrons. These changes should also become apparent in the variation of the magnetic susceptibility with x in the compounds $La_{1-x}Th_xAl_3$ and $Y_{1-x}Th_xAl_3$ when compared to $La_{1-x}Y_xAl_3$. In these compounds χ is mainly determined by Pauli paramagnetism of the conduction electrons and diamagnetism of conduction and core electrons. The room-temperature data for the above-mentioned ternary compounds are shown in Fig. 4. For the system $La_{1-x}Y_xAl_3$, the variation of χ with x remains limited by the two values indicated for $LaAl_3$ and YAl_3, whereas a very pronounced variation of χ with x is observed
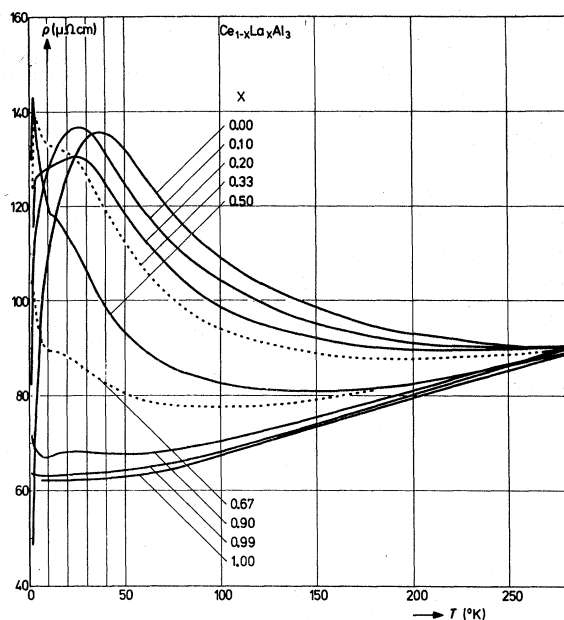

FIG. 1. Variation of the temperature dependence of the electrical resistivity ρ of $CeAl_3$ upon replacement of Ce by nonmagnetic La. The experimental curves have been shifted on the ρ scale so that they match at 300 °K. Some of the curves have been reproduced as broken lines in order to obtain a transparent figure.

for the Th compounds. For all compounds considered χ increases slightly with decreasing temperature. This is probably due to band-mixing effects and/or to the presence of small amounts of paramagnetic impurities. The variations of χ with x at room temperature, such as shown in Fig. 4, however, were found to remain essentially the same at 77 °K. The χ data for the systems $Y_{1-x}Th_xAl_3$ and $La_{1-x}Th_xAl_3$, therefore, suggest that, with increasing Th concentration, $N(E_F)$ first rises or is constant but then $(x > 0.3)$ decreases appreciably. Preliminary investigations, made by M. H. van Maaren of this laboratory, on the behavior of the electronic specific-heat coefficient γ in $Y_{1-x}Th_xAl_3$ as a function of x essentially corroborate the above interpretation of χ behavior.

III. CRYSTAL FIELD SPLITTING

Owing to the perturbing influence of the crystal field, the $2J+1$ degeneracy of the ground state of the Ce^{3+} ion is partly removed. In zero magnetic field this leads in the case of hexagonal symmetry to a splitting into three Kramers doublets. The localized magnetic moment now depends on the temperature through the Boltzmann average over these three doublets. The over-all splitting Δ of the ground-state manifold and the relative positions of the three doublets can be estimated with the help of the point-charge model. Actually, in cases where
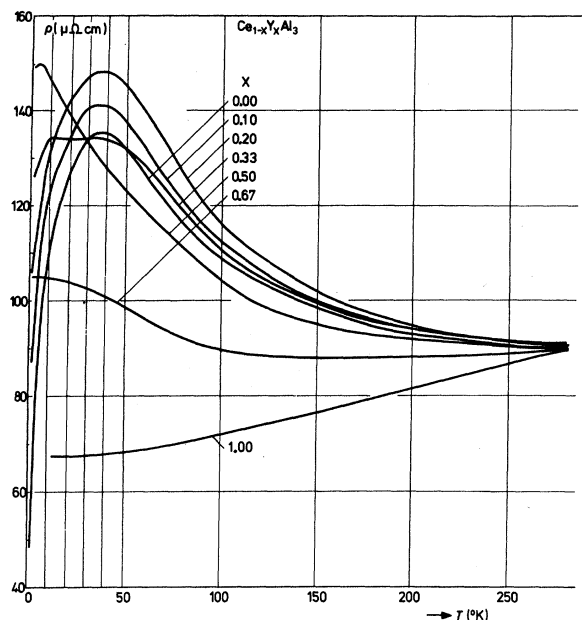
TABLE I. Lattice parameters for the binary hexagonal compounds considered in this paper.

Compound	Lattice constants (Å)		c/a
	a	c	
$CeAl_3$	6.545	4.609	0.704
$LaAl_3$	6.662	4.609	0.692
YAl_3	6.276[a]	4.582[a]	0.731[a]
$ThAl_3$	6.499	4.626	0.712

[a]D. M. Bailey, Acta Cryst. **23**, 729 (1967).

FIG. 2. Variation of the temperature dependence of the electrical resistivity ρ of $CeAl_3$ upon replacement of Ce by nonmagnetic Y (see also caption to Fig. 1).

FIG. 3. Variation of the temperature dependence of the electrical resistivity ρ of $CeAl_3$ upon replacement of Ce by nonmagnetic Th (see also caption to Fig. 1).

a direct comparison with experiment has been possible, this model proves to be rather unrealistic, especially with respect to estimates of the over-all splitting Δ. For the present compounds, we will nonetheless describe the crystal field splitting in terms of this model because it is well suited for discussion of the various possibilities.

The crystal field Hamiltonian, in its general form given by

$$H_c = \sum_{nm} B_n^m O_n^m \; ,$$

reduces, for the case of a Ce^{3+} ion in a hexagonal electric potential field, to

$$H_c = B_2^0 O_2^0 + B_4^0 O_4^0 \; . \tag{1}$$

Here O_2^0 and O_4^0 represent equivalent operators; the crystal field intensities, in the notation of Ref. 9, are given by

$$B_n^m = A_n^m \langle r^n \rangle \, \theta_n \; , \tag{2}$$

where

$$A_n^m = - |e| \; \frac{4}{2n+1} \sum_j \; q_j \; \frac{C_{nm}^2 f_{nm}(R_j)}{R_j^{2n+1}} \; . \tag{3}$$

In these expressions, $\langle r^n \rangle$ denotes the expectation value of the nth power of the modulus of the position vector of the $4f$ electron. θ_n represents the Stevens multiplicative factor, while q_j and R_j are the charge and the position of the surrounding ions, respectively. The constants C_{nm} and the expressions for the
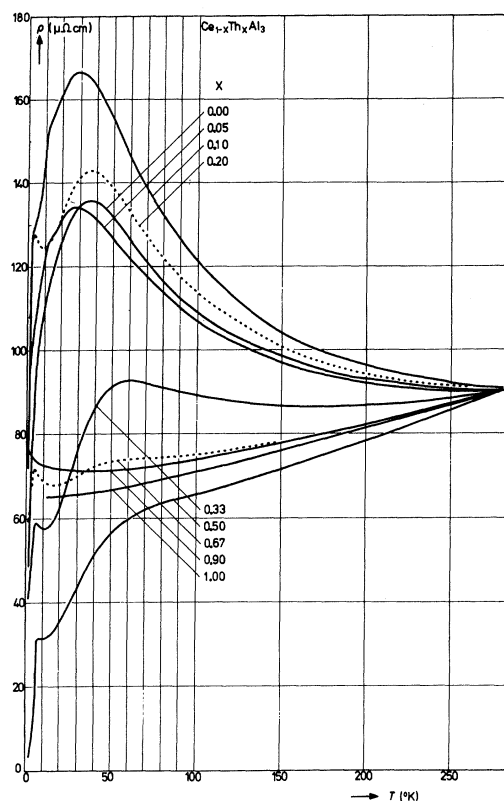
functions $f_{nm}(R)$ can be obtained from the data tabulated in Ref. 9. Putting $q_j = |e| \, Z_j$ and considering only the twelve nearest Al neighbors of the Ce^{3+} ion in $CeAl_3$, one finds

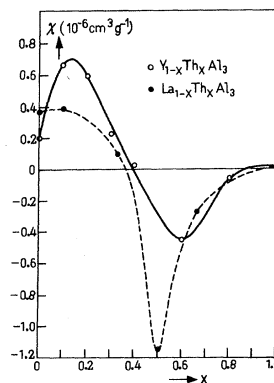$$B_2^0 = e^2 F(c/a) Z_{Al} \langle r^2 \rangle \, (\alpha/a^3) \; , \tag{4}$$

FIG. 4. Variation of the magnetic susceptibility χ of the compounds $Y_{1-x}Th_xAl_3$ as a function of composition. All data were taken at room temperature.
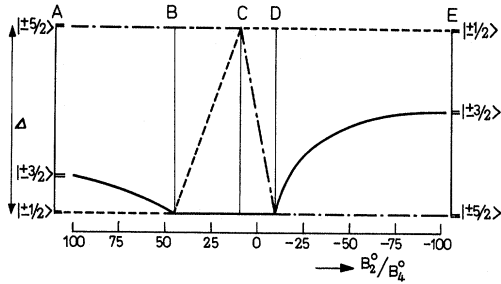
FIG. 5. Relative position of the three Kramers doublets of the split ground manifold of the Ce^{3+} ion in an hexagonal crystal field as a function of the ratio of the crystalline field intensities B_2^0 and B_4^0.

$$B_4^0 = e^2 F'(c/a) Z_{A1} \langle r^4 \rangle (\beta/a^3) , \qquad (5)$$

where F and F' are numerical constants for a given value of c/a, which, using the data for CeAl$_3$ of Table I, take the approximate values $-\frac{1}{2}$ and $+\frac{151}{64}$, respectively. It may be remarked that these values and the corresponding value of B_2^0/B_4^0 are at variance with those calculated by Mader and Swift.[10]

The relative position of the three doublet levels is determined by the ratio B_2^0/B_4^0. With the data listed for $\langle r^2 \rangle$, $\langle r^4 \rangle$, α, and β in Refs. 9 and 11, one finds $B_2^0/B_4^0 \simeq 110$. This corresponds to a relative position such as shown in the left-hand side of Fig. 5.

It will be shown in Sec. IV that the resistivity behavior depends rather strongly on the relative position of the three doublets in a given compound. Therefore, we have calculated these positions in Fig. 5 as a function of B_2^0/B_4^0 and will pursue further the study of crystal field effects by discussing the causes that will lead to changes in the B_2^0/B_4^0 ratio.

In the first place, we want to examine the influence of more distant neighbors: If account is also taken of the electric field due to the $(2+6)$ next-nearest Ce neighbors, one obtains, with $Z_{A1} = -1$ and $Z_{Ce} = +3$,[12,13] a value for B_2^0/B_4^0 close to -1300. Because of the insensitivity of the relative position of the levels towards B_2^0/B_4^0, when the latter quantity approaches the value -100, this corresponds to a level scheme as shown on the right-hand side of Fig. 5. We have also calculated the crystal field intensities due to the contributions of all atoms lying within a sphere of 10 Å centered around a Ce atom. Because in this case $B_2^0/B_4^0 \simeq -490$, the relative positions of the doublets are again the same as indicated on the right-hand side of Fig. 5. The latter calculation is considered to be more realistic than the former one, where account has been taken only of the nearest- and next-nearest-neighbor Al and Ce atoms. Actually, hardly any difference results in the final outcome if the radius of the sphere is extended from 10 to 20 Å. Summarizing, one

might say, therefore, that in going from left to right in Fig. 5, one passes from a level scheme corresponding to a crystal field caused by the nearest twelve Al neighbors to level schemes in which increasing account is taken of the influence of the remote Ce and Al atoms. In the above considerations, no proper account has been taken of screening effects. These can lead to effective electric charges at the Ce and Al sites which vary with the distance to the central Ce atom and may differ appreciably from those used above. This means that also B_2^0/B_4^0 values lying within $+100$ and -100 are not to be excluded a priori for CeAl$_3$, so that one has to deal with a whole scale of possible level schemes (see Fig. 5) for this compound.

Anticipating the results arrived at in one of the following sections, we want to mention that by means of the resistivity data of the compounds Ce$_{1-x}$La$_x$Al$_3$, Ce$_{1-x}$Y$_x$Al$_3$, and Ce$_x$Th$_{1-x}$Al$_3$, a choice can be made between the possibilities shown in Fig. 5. This choice becomes possible owing to the sensitivity of B_2^0/B_4^0 to the c/a ratio, and it is the latter ratio which can be changed by varying x in the above compounds. We have performed numerical calculations on the variation of B_2^0/B_4^0 as a function of c/a by taking account of contributions to the crystal field of all atoms lying within a sphere of 20 Å. These calculations show that if the c/a ratio is allowed to vary from 0.69 (LaAl$_3$) to approximately 0.73 (YAl$_3$), one has B_2^0/B_4^0 values varying from -350 to $-\infty$. These values are to be compared with $B_2^0/B_4^0 = -440$ obtained for $c/a = 0.704$ (CeAl$_3$). Clearly, La substitution in CeAl$_3$ produces a shift to the left on the B_2^0/B_4^0 scale in Fig. 5, whereas a shift in the opposite direction should be the result of Y or Th substitution. It has not been possible to check this behavior of B_2^0/B_4^0 as a function of c/a by numerical calculations for a situation in which screening effects are operative, although it is likely to apply in this case also.

IV. KONDO SIDEBAND MODEL

An essential feature of the Kondo exchange scattering[14] is the fact that it involves intermediate states of the localized spin which differ from the initial and/or from the final state: The eigenvalue of the z component of the localized spin moment in the intermediate state differs by one quantum from the eigenvalue proper to either the initial or the final state. When the localized spin can flip by one quantum without energy expenditure, the conduction electrons on the Fermi surface are scattered resonantly. For instance, for a localized moment with $S = \frac{1}{2}$, the $|+\frac{1}{2}\rangle$ and $|-\frac{1}{2}\rangle$ states are degenerate. In Kondo scattering, a flip from either $|+\frac{1}{2}\rangle$ to $|-\frac{1}{2}\rangle$ or vice versa always takes place, and this leads to a strong resonance at $T = 0$ in the transition probability $1/\tau_k$ for scattering of the conduction electrons

having energy E_k equal to E_F. The resonance peak broadens at $T \neq 0$ and with increasing temperature eventually disappears due to the diffuseness of the Fermi level.

In the present case, the situation is more complicated. Spin-flip scattering can occur in principle between the following sublevels of the ground-state manifold of the Ce^{3+} ion:

$$\langle \pm \tfrac{1}{2} | \leftrightarrow | \mp \tfrac{1}{2} \rangle , \quad \langle \pm \tfrac{1}{2} | \leftrightarrow | \pm \tfrac{3}{2} \rangle , \quad \langle \pm \tfrac{3}{2} | \leftrightarrow | \pm \tfrac{5}{2} \rangle .$$

In zero crystal field splitting, and in the absence of internal or external magnetic fields, each of these possibilities corresponds to elastic scattering and will lead to a resonance in the relaxation time for $E_k - E_F = 0$. In the presence of an hexagonal crystal field, elastic scattering is only possible for the first of the three possibilities. Maranzana[6] has shown that for each pair of doublets $\langle \pm \tfrac{1}{2} |, | \pm \tfrac{3}{2} \rangle$ or $\langle \pm \tfrac{3}{2} |, | \pm \tfrac{5}{2} \rangle$, Kondo exchange scattering leads to a sharp resonance peak at $T = 0$ in the transition probability $1/\tau_k$ at an energy shifted away from E_F, of an amount equal to the energy separation of the pair. These resonance peaks are designated as "Kondo sidebands." With increasing temperature, these Kondo sidebands broaden and eventually disappear owing to the Fermi level becoming diffuse. If the splitting of the Ce^{3+} manifold is such that the doublet $| \pm \tfrac{1}{2} \rangle$ is the highest level, the relaxation time at $T = 0$ does not even show the normal Kondo resonance at $E_k = E_F$ because, according to the Boltzmann distribution, the doublet is unoccupied at very low temperatures. In the two other cases the scattering is inelastic.

The interesting question is, of course, what sort of effects are to be expected in the resistivity-vs-temperature curve from a relaxation time containing resonances. Generally speaking, in order to obtain an expression of the resistivity as a function of temperature, the relaxation time must be introduced in the usual formula for the conductivity:

$$\sigma(T) \propto \int \tau_k(T, E_k) \, \frac{\partial f_k^0(\tau, E_k)}{\partial E_k} \, dE_k , \qquad (6)$$

where f_k^0 is the Fermi-Dirac distribution function in the absence of an applied electric field. When the relaxation time as a function of energy shows (as in this case) resonance peaks at $E_k \neq E_F$, one intuitively expects as a consequence of this the existence of two peaks in the resistivity-vs-temperature curve at temperatures equivalent to the distances of the energy levels in the two pairs of doublets. Numerical calculations of ρ as a function of T, based on Eq. (6), have been made for various positions of the doublets. The approximations used in the evaluation of Eq. (6) have been indicated in Ref. 6 (see also Ref. 15). The results of these calculations, as reported in Sec. V, indicate that

the peaks in the resistivity are usually shifted away, on the temperature scale, from the intuitively expected values. A number of factors bring about this shift: in particular, the derivative of the Fermi-Dirac distribution function and the temperature dependence of the relaxation time through the Boltzmann factors. A detailed study of the shifting of the resistivity peaks would require deriving Eq. (6) and putting this derivative equal to zero.

The width of the resistivity peaks is closely connected with the sharpness of the Fermi level at a given temperature. If the resonance scattering involves a large separation in energy between the crystal field levels, a rather diffuse Fermi level will be involved. For this reason, the resistivity maxima will, in general, become flatter the higher the temperature is at which they are observed.

V. INTERPRETATION OF RESISTIVITY DATA

The experimental ρ data presented in Sec. II (Figs. 1–3) will now be interpreted on the basis of the Kondo sideband model (see Sec. IV), employing the results of the calculations made on the crystal field splitting of the Ce^{3+} ground state (see Sec. III). In the numerical calculations of ρ as a function of T, it has been assumed that the total splitting of the Ce^{3+} ground state is a constant which is equivalent to 50 °K. Results for various relative positions of the three doublets corresponding to values of B_2^0/B_4^0 in the ranges ABC and CDE (see Fig. 5) are shown in Figs. 6 and 7, respectively. In these figures, just as in Fig. 8, only the relative differences in temperature behavior of ρ for the various crystal field splittings have relevance. The calculations have been performed in the limit of the validity of perturbation theory. In this limit, first- and second-order contributions to the relaxation time for scattering of the conduction electrons are of the same order of magnitude.

It is seen in Figs. 6 and 7 that above about 50 °K, ρ behavior in all situations is roughly the same, showing the increase of ρ with decreasing T expected in normal Kondo systems. This is because at temperatures sufficiently larger than the total splitting, the Ce^{3+} ground multiplet may be regarded as degenerate. Below about 50 °K, ρ behavior can be seen to differ appreciably in the various situations. At very low temperatures, ρ increases markedly with an increase of T except in region AB and at point D, where ρ decreases sharply with an increase of T. In the latter cases, the normal Kondo effect is present at very low temperatures also because the lowest state consists either of the doublet $| \pm \tfrac{1}{2} \rangle$ (region AB) or of the coinciding doublets $| \pm \tfrac{5}{2} \rangle$ and $| \pm \tfrac{3}{2} \rangle$ (point D). In these calculations the effect of sidebands becomes manifest in the presence of either one broad maximum if B_2^0/B_4^0 has values in the vicinity of A, C, or E or in the presence of
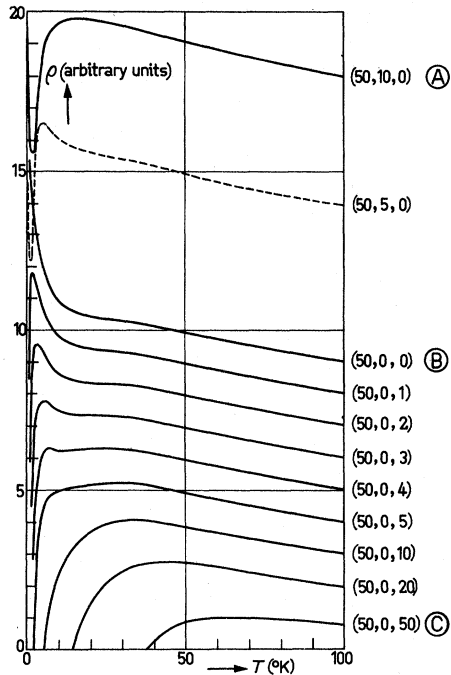
FIG. 6. Variation of the calculated temperature dependence of the electrical resistivity of CeAl$_3$ due to differences in relative position of the three doublets. The calculations include first- and second-order effects. The figures at the right-hand side represent the relative position (in °K) of the levels $|\pm\frac{5}{2}\rangle$, $|\pm\frac{3}{2}\rangle$, and $|\pm\frac{1}{2}\rangle$, respectively. The capital letters denote the corresponding situations in Fig. 5.

two maxima for values of B_2^0/B_4^0 near B or D. In the cases where two maxima are present, the one occurring at the lower temperature is seen to be the sharpest.

Calculations of only the first-order contribution to ρ as a function of T have also been made. The results for situations in the crystal field range CDE are shown in Fig. 8. It is interesting to note the anomalous behavior of ρ in a limited region beyond D. In that region, a minimum occurs in the ρ-T curve without the presence of a Kondo effect. An explanation of this anomaly can be found when one considers the influence on ρ behavior of the competing elastic and inelastic first-order scattering processes. Let us consider the situation where the $|\pm\frac{5}{2}\rangle$ doublet is the lowest state, separated by a small energy distance from the $|\pm\frac{3}{2}\rangle$ doublet, while the $|\pm\frac{1}{2}\rangle$ doublet is at a relatively high position [e.g., the situation (0, 1, 50) in Fig. 8]. With increasing temperature, starting at the lowest T, the initial increase of ρ is due to the influence of inelastic processes, involving transitions with spin flip between the doublets $|\pm\frac{5}{2}\rangle$ and $|\pm\frac{3}{2}\rangle$, accompanied by spin flip of the conduction electrons. At the same time, however, population of the $|\pm\frac{3}{2}\rangle$

doublet leads to a decrease of the effect of elastic scattering processes on ρ. This is because for each doublet this effect is proportional to the square of the expectation value of the z component of the relevant magnetic quantum number. The competing effect of elastic and inelastic scattering leads to a maximum in the ρ-T curve. In the partially reverse case [viz., (1, 0, 50), see Fig. 8], a maximum in the ρ-T curve is absent because elastic as well as inelastic scattering processes lead to an increase of ρ with T. In all cases of Fig. 8, at higher temperatures, the increase of ρ with T is due to the dominant influence of inelastic scattering processes, involving the pair of doublets $\langle\pm\frac{3}{2}|$, $|\pm\frac{1}{2}\rangle$.

When comparing experimental and theoretical results, it should be realized that in the latter results account has been taken only of magnetic effects with a constant concentration of scattering centers. Furthermore, the ratio between first- and second-order contribution to ρ has been restricted to the allowed limit. In the experimental results, the temperature dependence of ρ is influenced in addition by lattice vibrations, determining resistivity behavior, e.g., in LaAl$_3$, while the magnitude of the magnetic part is also influenced by dilution. Taking the above considerations into account, a considerable systematic resemblance can be seen between the sets of experimental curves presented in Figs. 1–3, on the one hand, and the sets of theoretical curves shown in Figs. 6 and 7,
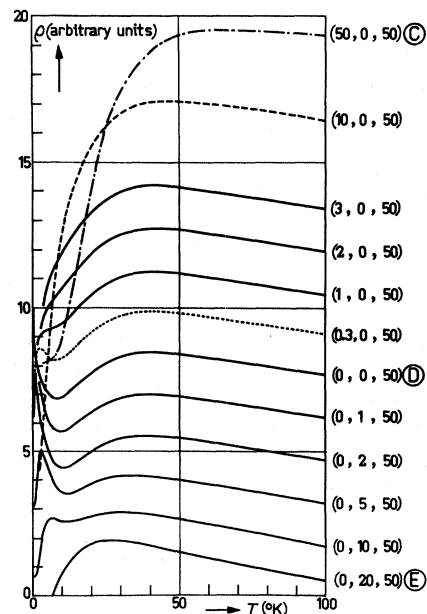

FIG. 7. Variation of the calculated temperature dependence of the electrical resistivity of CeAl$_3$ due to changes in the relative position of the crystal field levels (see also caption to Fig. 6).
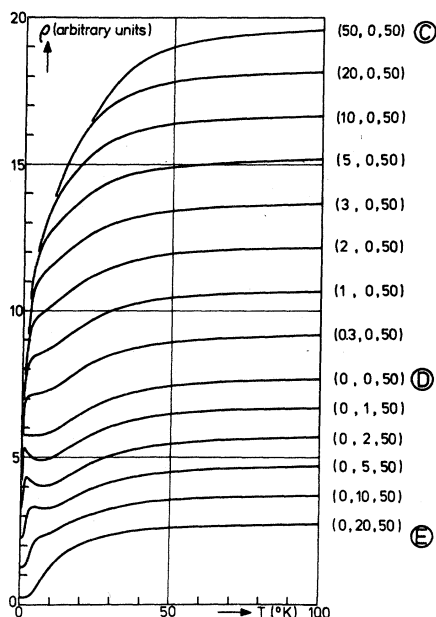
FIG. 8. Variation of the calculated temperature dependence of the electrical resistivity of $CeAl_3$ due to changes in relative position of the crystal field levels. In the calculations only first-order scattering effects are considered (see also caption to Fig. 6).

on the other, if it is assumed that in $CeAl_3$ the crystal field splitting of the Ce^{3+} ground state corresponds to the region around the point C in Fig. 5.

It has already been pointed out that in the set of compounds $Ce_{1-x}La_xAl_3$ the c/a ratio decreases with increasing x leading in Fig. 5 to a shift to the left on the B_2^0/B_4^0 scale (see Sec. III). The successive theoretical curves in Fig. 6, going from C to B, show a remarkable resemblance with the set of experimental curves obtained on $Ce_{1-x}La_xAl_3$ with increasing x (Fig. 1). This suggests that the crystal field splitting in $CeAl_3$ does indeed change through an increasing replacement of Ce by La, from a situation near point C to one near point B.

Partial replacement of Ce by Y leads to an increase in the c/a ratio and to a corresponding shift to the right on the B_2^0/B_4^0 scale in Fig. 5. In the successive theoretical curves of Fig. 7, when going from C to D, first one broad maximum remains present at about the same temperature. Only when approaching D, the presence of a second maximum at lower temperatures becomes clearly noticeable. In a limited region beyond the point D, this low-temperature maximum becomes enhanced. The set of experimental curves for $Ce_{1-x}Y_xAl_3$ with increasing x shows essentially the same trend of temperature dependence as sketched above (Fig. 2). With

x increasing from 0.00 to 0.20, the temperature dependence of ρ does not change appreciably, ρ behavior being characterized by one broad maximum. The presence of a second low-temperature maximum becomes visible for $x \geqslant 0.33$. Thus it seems plausible that substitution in $CeAl_3$ of Y for Ce leads to a change in the relative positions of the doublets from a situation near to point C to a situation slightly beyond D.

Confirmation of the above explanation of the change in ρ behavior upon dilution of $CeAl_3$ with YAl_3 can be obtained from the data for the set of $Ce_{1-x}Th_xAl_3$ compounds, although complications arise from the additional effect of Th substitution on the electronic density of states. Replacement in $CeAl_3$ of Ce by Th, just as by Y, leads to an increase of the c/a ratio, albeit smaller than in the case of Y substitution. When disregarding variations in the density of states, one may thus expect in the set of experimental curves for $Ce_{1-x}Th_xAl_3$, with increasing x, a trend of the temperature dependence similar to that of the theoretical set when going from C to or beyond D (see Fig. 7). The general trend in both sets of curves is indeed the same: With increasing x, likewise when going from C to D, there appears a second low-temperature maximum. In a further comparison, allowance should be made for the variation of $N(E_F)$. It has been suggested (see Sec. II) that in $Ce_{1-x}Th_xAl_3$ with x increasing from 0.00 to 0.30, $N(E_F)$ either goes through a maximum or is a constant, but then for $x > 0.3$ decreases appreciably. One might thus expect that Kondo sideband effects become enhanced in the region $0 < x < 0.3$ but weakened for x increasing above 0.3. There is a fairly good resemblance between the experimental curves with increasing x and the theoretical Kondo sideband curves of Fig. 7, when going from a point near C to somewhere near the situation $(0.3, 0, 50)$, if allowance is made of $N(E_F)$ first rising and then $(x > 0.3)$ decreasing appreciably. It is interesting to note that the experimental curve for the case of 67% Th shows very much the same temperature dependence as the theoretical first-order curves for situations immediately beyond point D, e.g., the curve marked $(0, 2, 50)$ in Fig. 8. This similarity might suggest that such a Th concentration does indeed bring the crystal field splitting into the region beyond D and, moreover, that due to the corresponding lowering of $N(E_F)$, Kondo sideband effects have totally disappeared. However, when considering the order of magnitude of first- and second-order effects (see Sec. VI), it appears that the above-mentioned similarity can only be accidental.

Let us summarize the above interpretation of ρ data. It is proposed that in $CeAl_3$ the hexagonal crystal field splits the Ce^{3+} ground state such that the doublet $|\pm\frac{3}{2}\rangle$ is the lowest and that either the

$|\pm\frac{5}{2}\rangle$ or the $|\pm\frac{1}{2}\rangle$ is the highest state. The total splitting is suggested as being of the order of 50 °K. The relative position of the levels is such that Kondo sideband effects lead to two resonant peaks in the resistivity, which merge together to one broad peak and correspond to the pairs of doublets $\langle\pm\frac{3}{2}|, |\pm\frac{1}{2}\rangle$ and $\langle\pm\frac{3}{2}|, |\pm\frac{5}{2}\rangle$. The normal Kondo effect due to the $|\pm\frac{1}{2}\rangle$ state is quenched at temperatures low in comparison to the total splitting because there this state is practically unoccupied.

Partial substitution of La for Ce, due to a decrease in the average c/a ratio, leads to a rearrangement of doublet levels such that ultimately the $|\pm\frac{1}{2}\rangle$ doublet closely approaches the ground-state $|\pm\frac{3}{2}\rangle$, while the position of the upper $|\pm\frac{5}{2}\rangle$ doublet remains essentially unaltered (see also Fig. 5). This leads to two well resolved resonance peaks in the $\rho-T$ curve, a sharp peak at low temperatures corresponding to the pair of doublets $\langle\pm\frac{3}{2}|,$ $|\pm\frac{1}{2}\rangle$ at a small energy distance, another broad one at higher temperatures, determined by the pair of doublets $\langle\pm\frac{3}{2}|, |\pm\frac{5}{2}\rangle$ at a larger energy distance.

Partial replacement of Ce by Y or Th, due to an increase of the average c/a ratio, ultimately leads either to the situation where the $|\pm\frac{5}{2}\rangle$ doublet is the lowest state with the $|\pm\frac{3}{2}\rangle$ doublet at a small energy distance (the case of Y) or to the reverse of this situation (the case of Th) while in all cases the $|\pm\frac{1}{2}\rangle$ doublet is the highest state. This leads, just as in the case of La substitution, to the occurrence of two resonant peaks in the $\rho-T$ curve. The low-temperature peak corresponds to the pair of doublets $\langle\pm\frac{3}{2}|, |\pm\frac{5}{2}\rangle$ at short energy distance, the high-temperature one to the pair of doublets $\langle\pm\frac{3}{2}|, |\pm\frac{1}{2}\rangle$ at a larger energy distance. In the set of compounds $Ce_{1-x}Th_xAl_3$, with increasing x, Kondo sideband effects are enhanced in the lower range of x values but weakened in the higher range due to the corresponding variation of the electronic density of states at the Fermi level.

VI. CONCLUDING REMARKS

In the above calculations, a value of 50 °K has been assumed for the over-all splitting of the ground-state manifold of the Ce^{3+} ions due to the crystalline electric field. This value is to be considered as approximate. Furthermore, it should be somewhat smaller and larger for high x values of the compounds $Ce_{1-x}La_xAl_3$ and $Ce_{1-x}Y_xAl_3$, respectively. Assuming a somewhat different value for B_2^0/B_4^0, an appreciably higher estimate (280 °K) of the over-all splitting for $CeAl_3$ has been given by Mader and Swift[10] by means of the comparison of a calculated and the experimental curve of the reciprocal susceptibility vs temperature. The observed deviations from Curie-Weiss behavior are slight and occur only below 50 °K. Therefore,

this method is rather insensitive and in addition would give rise to an overestimate, as deviations from Curie-Weiss behavior may also arise due to the presence of a Kondo effect.[16]

It has been shown in Secs. I–V that the Kondo sideband concept is able to account satisfactorily for the remarkable temperature dependence observed in the electrical resistivity of the compound $CeAl_3$ and, in addition, proves to be able to deal adequately with the changes in ρ behavior introduced upon partial replacement of Ce by La, Y, or Th. We consider these facts as strong evidence for the validity of the Kondo sideband concept.

It has still to be considered whether the Kondo sideband model can account also for the magnitude of the magnetic resistivity. In the theory (see Ref. 6), the first-order transition probability for scattering is given by the relation

$$\frac{1}{\tau^{(1)}} = C\Gamma^2 N(E_F)f^{(1)}, \tag{7}$$

while for the second-order transition holds

$$\frac{1}{\tau^{(2)}} = C|\Gamma|^3 N^2(E_F)f^{(2)}. \tag{8}$$

In Eqs. (7) and (8), C is a constant, Γ the effective s-f exchange integral, $N(E_F)$ the electronic density of states, $f^{(1)}$ and $f^{(2)}$ functions of temperature, and crystal field splitting of the Ce^{3+} ground state. The factor $C\Gamma^2 N(E_F)$, figuring in both equations, has been disregarded in the calculations, so that the first-order contribution to resistivity $\rho^{(1)}$ is independent of Γ and $N(E_F)$, while the second-order contribution $\rho^{(2)}$ is proportional to $|\Gamma|N(E_F)$. The calculations have been performed in the limit of the validity of second-order perturbation theory, i.e., the maximum contributions to $\rho^{(1)}$ and $\rho^{(2)}$ have been given equal magnitude. It appeared from the relative magnitudes of $f^{(1)}$ and $f^{(2)}$ that in this limit one has $|\Gamma|N(E_F)\simeq 0.1$. A rough estimate of the magnitude of $\rho^{(1)}$ in $CeAl_3$ can be obtained from the experimental data. It is seen in Fig. 1, at the low-temperature side, that the lowest values for $CeAl_3$ and $LaAl_3$ differ by about 10 $\mu\Omega$ cm. This value constitutes a reasonable measure for $\rho^{(1)}$ because the residual value for $CeAl_3$ seems to be almost reached, while, moreover, the second-order contribution appears to be small at high temperatures, where the $CeAl_3$ and $LaAl_3$ curves have been matched. On the other hand, it appears from Fig. 1 that the maximum contribution in $CeAl_3$ to $\rho^{(2)}$ is about 100 $\mu\Omega$cm. Thus, in the experiment $\rho^{(2)}$ is an order of magnitude larger than $\rho^{(1)}$. One might then conclude that in $CeAl_3$ the produce $|\Gamma|N(E_F)$ should have a value of about unity. This conclusion is admitted only as far as the extrapolation of perturbation theory beyond the limits of its validity is allowed. The conclu-

sion that $|\Gamma| N(E_F) \simeq 1$ does not seem unreasonable. It follows from Knight-shift data for CeAl$_3$[4,5] that $\Gamma \simeq -3$ eV/at., whereas $N(E_F)$ can be close to 0.5 state/eV at., so that one finally arrives at the correct order of magnitude of the product $|\Gamma| N(E_F)$. Moreover, with the above values for Γ and $N(E_F)$ and using the conventional equation for spin-disorder resistivity, one arrives at a value of about 10 $\mu\Omega$cm for $\rho^{(1)}$ for temperatures relatively high compared to the total crystal field splitting. This is consistent with the above estimate of $\rho^{(1)}$ from experimental data. It follows that one "arbitrary unit," used in the theoretical first-order results (see Fig. 8), is equivalent to about 1 $\mu\Omega$cm. It also follows, then, that in the case of Ce$_{0.33}$Th$_{0.67}$Al$_3$ in the low-temperature region, the total variation of ρ in the experiment is at least one order of magnitude larger than expected from the first-order contribution in the situation

(0, 2, 50) (compare the results of Figs. 3 and 8). In this case, too, the second-order contribution evidently remains dominant.

An alternative way to explain a decrease of ρ with increasing T seems possible, in principle, by means of Blatt's mechanism.[17] In that case, the $4f^1$ level has to be close to the Fermi surface, which is not unlikely. To obtain a maximum in the ρ-vs-T curve the Blatt mechanism has to be combined with effects of different origin (for instance, crystal field effects, if these could be treated simultaneously with the Blatt mechanism). It is seriously doubted, however, whether in such a model the occurrence of two maxima in the ρ-T curve could be explained, and whether the ρ data obtained for CeAl$_3$ upon increasing replacement of Ce by La, Y, or Th could consistently be accounted for.

[1]K. H. J. Buschow and H. J. van Daal, Phys. Rev. Letters 23, 408 (1969).

[2]H. J. van Daal and K. H. J. Buschow, Phys. Letters 31A, 103 (1970).

[3]K. H. J. Buschow and H. J. van Daal, Solid State Commun. 8, 363 (1970).

[4]A. M. van Diepen, H. W. de Wijn, and K. H. J. Buschow, J. Chem. Phys. 46, 3489 (1967).

[5]H. W. de Wijn, K. H. J. Buschow, and A. M. van Diepen, Phys. Status Solidi 30, 759 (1968).

[6]F. E. Maranzana, Phys. Rev. Letters 25, 239 (1970).

[7]J. H. N. van Vucht and K. H. J. Buschow, J. Less-Common Metals 10, 98 (1965).

[8]H. J. van Daal and K. H. J. Buschow, Solid State Commun. 7, 217 (1969).

[9]M. T. Hutchings, in Solid State Physics, edited by F. Seitz and D. Turnbull (Academic, New York, 1964), Vol. 16, p. 227.

[10]K. H. Mader and W. M. Swift, J. Phys. Chem. Solids 29, 1759 (1968).

[11]A. J. Freeman and R. E. Watson, in Magnetism IIA, edited by G. T. Rado and H. Suhl (Academic, New York, 1965), p. 292.

[12]J. A. White, H. J. Williams, J. H. Wernick, and R. G. Sherwood, Phys. Rev. 131, 1039 (1963).

[13]H. W. de Wijn, A. M. van Diepen, and K. H. J. Buschow, Phys. Rev. B 1, 4203 (1970).

[14]J. Kondo, Progr. Theoret. Phys. (Kyoto) 32, 37 (1964).

[15]F. E. Maranzana and P. Bianchessi, Phys. Status Solidi (to be published).

[16]M. D. Daybell and W. A. Steyert, Rev. Mod. Phys. 40, 380 (1968).

[17]F. J. Blatt, J. Phys. Chem. Solids 17, 177 (1961).

Accurate-Pairing Treatment of the Coulomb Interaction in the Anderson Model of a Localized Moment in a Metal*

R. H. Parmenter
Department of Physics, University of Arizona, Tucson, Arizona 85721
(Received 6 August 1970)

The treatment of the Anderson model of a localized moment in a metal has been extended beyond the effective-field approximation by a method recently developed for studying the Hubbard model. This leads to an accurate treatment of the Coulomb interaction associated with the localized center. The results are a simple generalization of those obtained by Anderson within the context of the effective-field approximation.

I. INTRODUCTION

In a previous paper, the author[1] studied the problem of an interacting system of localized moments

in a dilute magnetic alloy. Each localized center containing a magnetic moment was represented by the model of Anderson.[2] The problem was treated by means of an equation-of-motion method, includ-